

A strong coupling critique of spin fluctuation driven charge order in underdoped cuprates

Vivek Mishra and M. R. Norman

Materials Science Division, Argonne National Laboratory, Argonne, IL 60439

(Dated: December 3, 2024)

Charge order has emerged as a generic feature of doped cuprates, leading to important questions about its origin and its relation to superconductivity. Recent experiments on two classes of hole doped cuprates indicate a novel d-wave symmetry for the order. These were motivated by earlier spin fluctuation theoretical studies based on an expansion about hot spots in the Brillouin zone that indicated such order would be competitive with d-wave superconductivity. Here, we reexamine this problem by solving strong coupling equations in the full Brillouin zone. Our results find that bond-oriented order, as seen experimentally, is strongly suppressed, indicating that the charge order must have a different origin.

PACS numbers: 74.72.-h, 75.25.Dk, 71.45.Lr, 74.20.Mn

Following earlier NMR studies [1], recent x-ray experiments on underdoped cuprates have detected short range charge density wave (CDW) order with a period of 3 to 5 lattice spacings in YBCO [2–4], and in Bi based [5, 6] and Hg based cuprates [7]. For YBCO, the doping range where the charge order has been observed [8] coincides with the doping range where quantum oscillation experiments detect reconstruction of the Fermi surface [9]. In conventional CDW systems, the charge order is thought to have s-wave symmetry [10]. In contrast, scanning tunneling microscopy [11] and resonant soft x-ray scattering [12, 13] data have revealed a novel d-wave symmetry, where the two oxygen ions in a CuO_2 unit are out of phase. This charge order differs from the more robust magnetic stripe order seen earlier in La based compounds [14–16], which appears to have s-wave symmetry instead [13]. In all cases, though, the wavevector is oriented along the bond direction [17].

The search for d-wave symmetry was motivated by earlier theoretical studies of Metlitski and Sachdev [18, 19]. They have shown that charge order is competitive with d-wave superconductivity in a spin fluctuation model. This instability has a d-wave form factor, with a diagonal wavevector that spans Fermi surface points (hot spots) that intersect the antiferromagnetic zone boundary of the undoped phase (Fig. 1). The subsequent observation of charge order in YBCO motivated a number of follow up studies [20–23]. Most of these rely on an expansion around the hot spots, with the Fermi surface curvature treated as a perturbation. So, the question arises whether these results survive in the strong coupling limit with the full Brillouin zone taken into account.

Here, we use full Brillouin zone Eliashberg theory to study the charge order instability. This formalism has been used in the past to study d-wave superconductivity originating from spin fluctuations [24, 25]. It has also been used to study instabilities in the particle-hole channel [26]. Recently, this formalism was used by us to examine the effect of the pseudogap on spin-fluctuation

mediated pairing [27].

Our starting point is the linearized equation for the anomalous self energy in the particle-hole channel

$$T \sum_{k', \omega_m} V(k - k', i\omega_n - i\omega_m) \mathcal{P}^Q(k', i\omega_m) \Phi^Q(k', i\omega_m) = \lambda \Phi^Q(k, i\omega_n). \quad (1)$$

Here Q is the ordering vector, V is the interaction and \mathcal{P}^Q is the CDW particle-hole kernel

$$\mathcal{P}^Q(k', i\omega_m) = G(k' - \frac{Q}{2}, i\omega_m) G(k' + \frac{Q}{2}, i\omega_m) \quad (2)$$

where $G(k, i\omega) = (i\omega - \xi_k)^{-1}$ is the fermionic Green's function. We consider a dispersion (ξ_k) that fits ARPES data for $\text{Bi}_2\text{Sr}_2\text{CaCu}_2\text{O}_{8+\delta}$ (tb2 dispersion of Ref. 28).

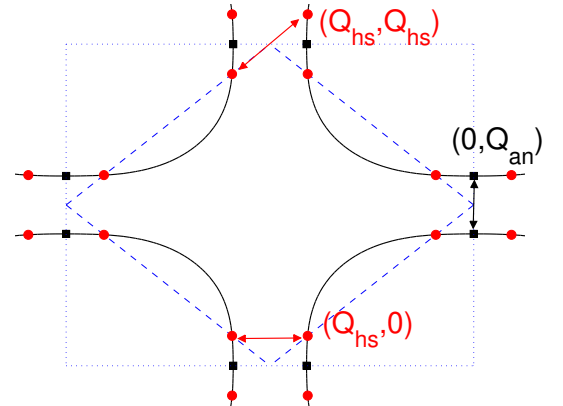


FIG. 1: (Color online) Fermi surface for the tight binding dispersion considered in this work. The dashed lines show the antiferromagnetic Brillouin zone and the dotted lines the structural one. Filled circles denote the hot spots and filled squares the antinodal points. The wavevectors studied here are indicated by the arrows.

The interaction assumed here is

$$V(k, i\Omega_n) = \int_{-\infty}^{\infty} \frac{dx}{\pi} \frac{V''(k, x)}{i\Omega_n - x} \quad (3)$$

where V'' is proportional to the imaginary part of the dynamic spin susceptibility. We consider the phenomenological form [29]

$$V''(k, \Omega) = \frac{3}{2} g_{sf}^2 \chi_Q \frac{\Omega \Omega_{sf}}{\chi_k^2 \Omega_{sf}^2 + \Omega^2}$$

$$\chi_k = (\xi_{AF}/a)^{-2} + 2 + \cos k_x a + \cos k_y a \quad (4)$$

where g_{sf} is the spin-fermion coupling constant, ξ_{AF} is the antiferromagnetic correlation length, χ_Q is the static susceptibility at $Q_{AF} = (\pi/a, \pi/a)$ and Ω_{sf} is the characteristic spin-fluctuation energy scale. Because of the $1/\Omega$ decay of V'' , we impose a frequency cut-off, Ω_c . We use $\Omega_c = 300$ meV, $\Omega_{sf} = 100$ meV, $g_{sf}^2 \chi_Q = 0.9$ eV and $\xi_{AF} = 2a$, where a is the lattice constant. The values of ξ_{AF} and Ω_{sf} are motivated from inelastic neutron scattering studies of the magnetic excitations of underdoped YBCO near Q_{AF} [30, 31]. Ω_c is motivated from recent resonant inelastic x-ray scattering studies of the higher energy excitations away from Q_{AF} [32, 33]. The value of $g_{sf}^2 \chi_Q$ was chosen to obtain a superconducting T_c of 50 K, typical for underdoped YBCO. At the transition, the leading eigenvalue λ in Eq. (1) reaches 1, with its eigenvector giving the structure of the CDW order parameter.

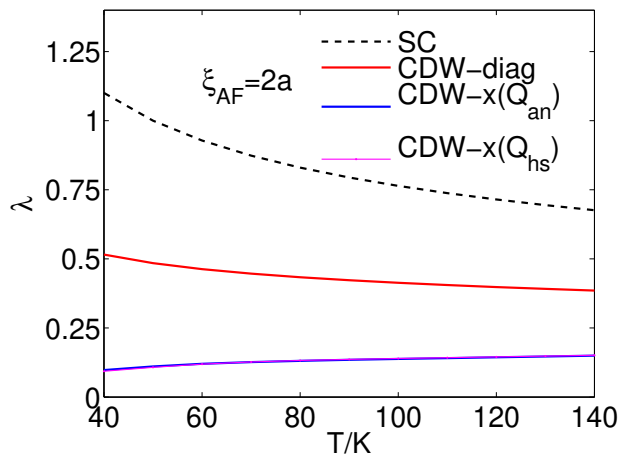


FIG. 2: (Color online) Temperature dependence of the leading eigenvalues for the superconducting d-wave state (SC), the diagonal CDW state (CDW-diag) and the bond oriented CDW state (CDW-x). The ordering vector for CDW-diag is (Q_{hs}, Q_{hs}) . For CDW-x, two vectors were considered: $(Q_{an}, 0)$ and $(Q_{hs}, 0)$.

We consider the CDW instabilities for the diagonal CDW case (CDW-diag) with ordering vector (Q_{hs}, Q_{hs}) , and for the bond oriented case (CDW-x) with vectors $(Q_{an}, 0)$ and $(Q_{hs}, 0)$, as shown in Fig. 1. We perform our calculations with a $0.02\pi/a$ momentum grid with 16

Matsubara frequencies, which is sufficient for convergence of the eigenvalues for the temperature range studied here (see supplementary information). Fig. 2 shows the temperature dependence of the leading eigenvalue for the different CDW cases along with the d-wave superconducting case.

As expected, the eigenvalue for the superconducting case exhibits a logarithmic divergence in T . This is present as well for CDW-diag order, though we find it to be significantly reduced relative to the superconducting one. The CDW-diag state has d-wave (B_{1g}) symmetry with a momentum dependence that is well described by $\cos(k_x a) - \cos(k_y a)$ as can be seen in Fig. 3 (a). Increasing the antiferromagnetic coherence length doesn't change our findings. The CDW-diag instability becomes stronger with longer ξ_{AF} , but it always remains subdominant relative to d-wave superconductivity (supplementary information).

We now focus on the bond-oriented CDW states, since there is no experimental evidence for diagonal-oriented order. The T dependence of the leading eigenvalues for CDW-x are also plotted in Fig. 2. They are almost identical for vectors $(Q_{hs}, 0)$ and $(Q_{an}, 0)$. The eigenvalues vary little with temperature, showing no evidence for a log in the temperature range studied. This is one of our main results, and differs from an analytic approximation quoted in earlier work [23]. We believe the lack of a log divergence is due to the fact that, unlike the diagonal case, a bond-oriented wavevector provides nesting for only half the pairs of hot spots [34].

We next look at the structure of the CDW-x state. Fig. 3 (b) shows the momentum dependence of the eigenvector corresponding to the leading eigenvalue, and can be well fit by a sum of a constant (s), $\cos(k_x a) + \cos(k_y a)$ (s') and $\cos(k_x a) - \cos(k_y a)$ (d), with the d-wave component dominant, consistent with earlier studies [21].

Our results cast doubt on a spin fluctuation mediated origin for the observed charge order. On the other hand, the dependence of the observed wavevector on doping [8] is suggestive that the Fermi surface is playing some role as in classic CDW systems. This is in contrast to the La based cuprates whose doping dependence is opposite to this, as would be expected from a real space picture where the wavevector is proportional to the doping. In classic CDW systems like $2H\text{-NbSe}_2$, phonons play an important role [35]. This may be the case in the cuprates as well, where anomalies have been seen in both optic [36] and acoustic [37] phonon modes near the charge ordering vector. It is interesting to note that B_{1g} phonon modes have been postulated to be responsible for dispersion anomalies seen in photoemission near the antinodes [38], and perhaps their d-wave symmetry is related to that of the charge order. In support of this, several theoretical studies have suggested that coupling of the electrons to such modes can cause d-wave charge order [39, 40]. This does not mean that spin mediated interactions are completely

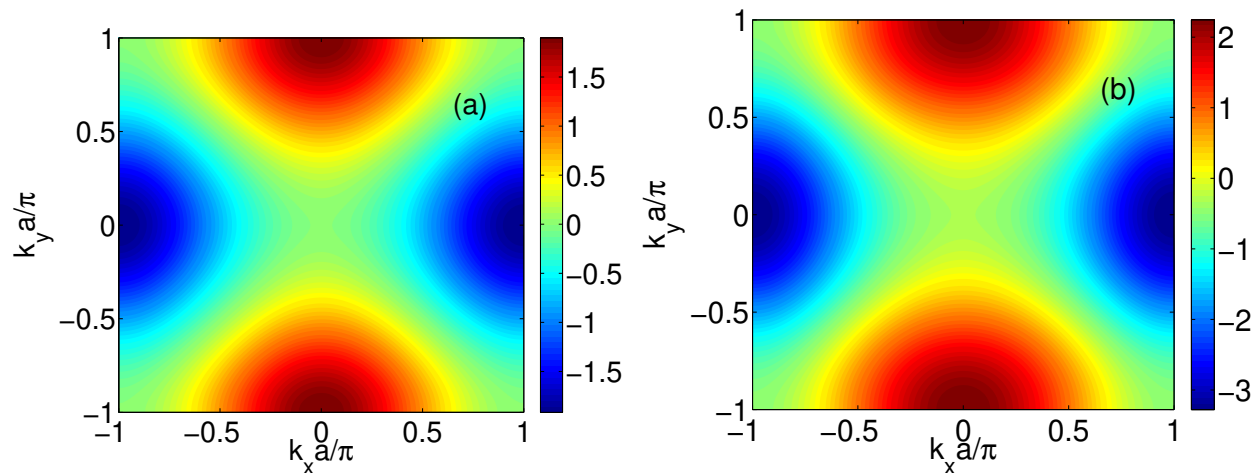


FIG. 3: (Color online) The momentum dependence of the eigenvectors at the lowest Matsubara frequency ($T=40$ K) corresponding to leading eigenvalues for the (a) CDW-diaq and (b) CDW-x states. For CDW-x, the ordering vector is $(Q_{an}, 0)$, though the eigenvector for $(Q_{hs}, 0)$ is similar. A normalization condition of $T \sum_{\omega_n, k} |\Phi^Q(k, i\omega_n)|^2 = 1$ is employed.

irrelevant for the charge order, but our results indicate they are unlikely to be the driving force.

This work was supported by the Center for Emergent Superconductivity, an Energy Frontier Research Center funded by the US DOE, Office of Science, under Award No. DE-AC0298CH1088. We gratefully acknowledge the computing resources provided on Blues and Fusion, the high-performance computing clusters operated by the Laboratory Computing Resource Center at Argonne National Laboratory.

[1] T. Wu, H. Mayaffre, S. Kramer, M. Horvatic, C. Berthier, W. N. Hardy, R. Liang, D. A. Bonn and M.-H. Julien, *Nature* **477**, 191 (2011).

[2] G. Ghiringhelli, M. Le Tacon, M. Minola, S. Blanco-Canosa, C. Mazzoli, N. B. Brookes, G. M. De Luca, A. Frano, D. G. Hawthorn, F. He, T. Loew, M. M. Sala, D. C. Peets, M. Salluzzo, E. Schierle, R. Sutarto, G. A. Sawatzky, E. Weschke, B. Keimer and L. Braicovich, *Science* **337**, 821 (2012).

[3] J. Chang, E. Blackburn, A. T. Holmes, N. B. Christensen, J. Larsen, J. Mesot, R. Liang, D. A. Bonn, W. N. Hardy, A. Watenphul, M. V. Zimmermann, E. M. Forgan and S. M. Hayden, *Nature Phys.* **8**, 871 (2012).

[4] A. J. Achkar, R. Sutarto, X. Mao, F. He, A. Frano, S. Blanco-Canosa, M. Le Tacon, G. Ghiringhelli, L. Braicovich, M. Minola, M. Moretti Sala, C. Mazzoli, R. Liang, D. A. Bonn, W. N. Hardy, B. Keimer, G. A. Sawatzky and D. G. Hawthorn, *Phys. Rev. Lett.* **109**, 167001 (2012).

[5] R. Comin, A. Frano, M. M. Yee, Y. Yoshida, H. Eisaki, E. Schierle, E. Weschke, R. Sutarto, F. He, A. Soumyanarayanan, Y. He, M. Le Tacon, I. S. Elfimov, J. E. Hoffman, G. A. Sawatzky, B. Keimer and A. Damascelli, *Science* **343**, 390 (2014).

[6] E. H. da Silva Neto, P. Aynajian, A. Frano, R. Comin, E. Schierle, E. Weschke, A. Gyenis, J. Wen, J. Schneeloch, Z. Xu, S. Ono, G. Gu, M. Le Tacon and A. Yazdani, *Science* **343**, 39 (2014).

[7] W. Tabis, Y. Li, M. L. Tacon, L. Braicovich, A. Kreyssig, M. Minola, G. Dellea, E. Weschke, M. J. Veit, M. Ramazanoglu, A. I. Goldman, T. Schmitt, G. Ghiringhelli, N. Barisic, M. K. Chan, C. J. Dorow, G. Yu, X. Zhao, B. Keimer and M. Greven, *Nature Comm.* **5**, 5875 (2014).

[8] S. Blanco-Canosa, A. Frano, E. Schierle, J. Porras, T. Loew, M. Minola, M. Bluschke, E. Weschke, B. Keimer and M. Le Tacon, *Phys. Rev. B* **90**, 054513 (2014).

[9] S. E. Sebastian, N. Harrison and G. G. Lonzarich, *Rep. Prog. Phys.* **75**, 102501 (2012).

[10] G. Gruner, *Rev. Mod. Phys.* **60**, 1129 (1988).

[11] K. Fujita, M. H. Hamidian, S. D. Edkins, C. K. Kim, Y. Kohsaka, M. Azuma, M. Takano, H. Takagi, H. Eisaki, S. Uchida, A. Allais, M. J. Lawler, E.-A. Kim, S. Sachdev and J. C. S. Davis, *Proc. Natl. Acad. Sci.* **111**, 3026 (2014).

[12] R. Comin, R. Sutarto, F. He, E. da Silva Neto, L. Chauviere, A. Frano, R. Liang, W. N. Hardy, D. A. Bonn, Y. Yoshida, H. Eisaki, J. E. Hoffman, B. Keimer, G. A. Sawatzky and A. Damascelli, arXiv:1402.5415.

[13] A. J. Achkar, F. He, R. Sutarto, C. McMahan, M. Zwiebler, M. Hucker, G. D. Gu, R. Liang, D. A. Bonn, W. N. Hardy, J. Geck and D. G. Hawthorn, arXiv:1409.6787.

[14] J. M. Tranquada, B. J. Sternlieb, J. D. Axe, Y. Nakamura and S. Uchida, *Nature* **375**, 561 (1995).

[15] Y.-J. Kim, G. D. Gu, T. Gog and D. Casa, *Phys. Rev. B* **77**, 064520 (2008).

[16] M. Hucker, M. v. Zimmermann, G. D. Gu, Z. J. Xu, J. S. Wen, G. Xu, H. J. Kang, A. Zheludev and J. M. Tranquada, *Phys. Rev. B* **83**, 104506 (2011).

[17] For lightly doped La based cuprates, diagonal charge order is seen.

[18] M. A. Metlitski and S. Sachdev, *Phys. Rev. B* **82**, 075128 (2010).

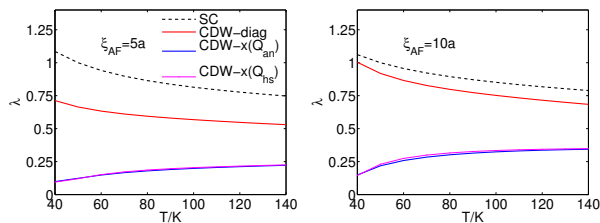
[19] M. A. Metlitski and S. Sachdev, *New J. Phys.* **12**, 105007 (2010).

- [20] K. B. Efetov, H. Meier and C. Pepin, *Nature Phys.* **9**, 442 (2013).
- [21] S. Sachdev and R. La Placa, *Phys. Rev. Lett.* **111**, 027202 (2013).
- [22] A. Allais, J. Bauer and S. Sachdev, *Phys. Rev. B* **90**, 155114 (2014).
- [23] Y. Wang and A. Chubukov, *Phys. Rev. B* **90**, 035149 (2014).
- [24] P. Monthoux and D. Pines, *Phys. Rev. Lett.* **69**, 961 (1992).
- [25] D. J. Scalapino, *Rev. Mod. Phys.* **84**, 1383 (2012).
- [26] N. Bulut, D. J. Scalapino and S. R. White, *Phys. Rev. B* **47**, 14599 (1993).
- [27] V. Mishra, U. Chatterjee, J. C. Campuzano and M. R. Norman, *Nature Phys.* **10**, 357 (2014).
- [28] M. R. Norman, *Phys. Rev. B* **75**, 184514 (2007).
- [29] A. J. Millis, H. Monien and D. Pines, *Phys. Rev. B* **42**, 167 (1990).
- [30] H. F. Fong, P. Bourges, Y. Sidis, L. P. Regnault, J. Bossy, A. Ivanov, D. L. Milius, I. A. Aksay and B. Keimer, *Phys. Rev. B* **61**, 14773 (2000).
- [31] P. Dai, H. A. Mook, R. D. Hunt and F. Dogan, *Phys. Rev. B* **63**, 054525 (2001).
- [32] M. Le Tacon, G. Ghiringhelli, J. Chaloupka, M. Moretti Sala, V. Hinkov, M. W. Haverkort, M. Minola, M. Bakr, K. J. Zhou, S. Blanco-Canosa, C. Monney, Y. T. Song, G. L. Sun, C. T. Lin, G. M. De Luca, M. Salluzzo, G. Khaliullin, T. Schmitt, L. Braicovich, B. Keimer, *Nature Physics* **7**, 725 (2011).
- [33] M. P. M. Dean, A. J. A. James, R. S. Springell, X. Liu, C. Monney, K. J. Zhou, R. M. Konik, J. S. Wen, Z. J. Xu, G. D. Gu, V. N. Strocov, T. Schmitt, and J. P. Hill, *Phys. Rev. Lett.* **110**, 147001 (2013).
- [34] H. J. Schulz, *Phys. Rev. Lett.* **64**, 1445 (1990).
- [35] F. Weber, S. Rosenkranz, J.-P. Castellán, R. Osborn, R. Hott, R. Heid, K.-P. Bohnen, T. Egami, A. H. Said and D. Reznik, *Phys. Rev. Lett.* **107**, 107403 (2011).
- [36] D. Reznik, *Physica C* **481**, 75 (2012).
- [37] M. Le Tacon, A. Bosak, S. M. Souliou, G. Dellea, T. Loew, R. Heid, K.-P. Bohnen, G. Ghiringhelli, M. Krisch and B. Keimer, *Nature Phys.* **10**, 52 (2014).
- [38] T. Cuk, F. Baumberger, D. H. Lu, N. Ingle, X. J. Zhou, H. Eisaki, N. Kaneko, Z. Hussain, T. P. Devereaux, N. Nagaosa and Z.-X. Shen, *Phys. Rev. Lett.* **93**, 117003 (2004).
- [39] H. C. Fu, C. Honerkamp and D.-H. Lee, *EPL* **75**, 146 (2006).
- [40] D. M. Newns and C. C. Tsuei, *Nature Phys.* **3**, 184 (2007).

Supplementary material

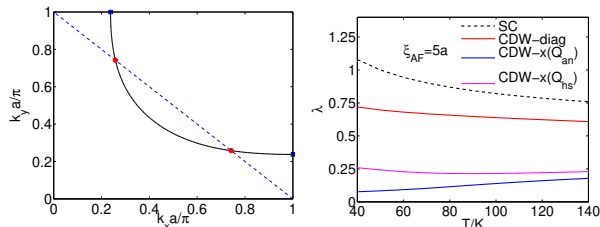
Effect of a larger antiferromagnetic coherence length

Supplementary Fig. 1 shows the effect of a larger antiferromagnetic correlation length. We use the same parameters for interactions as for $\xi_{AF} = 2a$, except for the overall prefactor $g_{sf}^2 \chi_Q$, which we set to 0.49 eV and 0.35 eV for $\xi_{AF} = 5a$ and $10a$, respectively, in order to obtain a superconducting T_c of 50 K. As can be seen, increasing the antiferromagnetic correlation length leads to similar results to those presented in the main text for $\xi_{AF} = 2a$.



Supplementary Fig. 1: Temperature dependence of the leading eigenvalues for the superconducting (SC), diagonal CDW (CDW-diag) and bond-oriented CDW (CDW-x) states, for $\xi_{AF} = 5a$ and $10a$.

Effect of the band structure on the CDW order



Supplementary Fig. 2: Fermi surface for the alternate fermionic dispersion is shown in the left panel. The right one shows the temperature dependence of the leading eigenvalue for the superconducting (SC), diagonal CDW (CDW-diag), and bond-oriented CDW (CDW-x) states for ordering vectors Q_{hs} and Q_{an} .

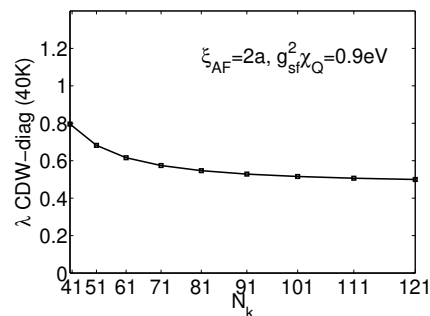
We study a different fermionic dispersion where Q_{an} and Q_{hs} are further separated than in the previous dispersion to test how this influences the solutions at $(Q_{an}, 0)$ and $(Q_{hs}, 0)$. Supplementary Fig. 2 shows the Fermi surface for this alternate band structure and the resulting temperature dependence of the leading eigenvalues for various CDW states. Here we use $\xi_{AF} = 5a$ and keep the rest of the parameters for the interaction as before, except again we adjust $g_{sf}^2 \chi_Q$ to 0.73 eV in order

to obtain a superconducting T_c of 50 K. The fermionic dispersion is

$$\xi(k_x, k_y) = 0.4 (\cos k_x a + \cos k_y a) - 0.32 \cos k_x a \cos k_y a + 0.04 (\cos 2k_x a + \cos 2k_y a) - 0.15 \quad (5)$$

where all energy scales are in eV. For this dispersion, we can clearly see that the eigenvalues of the CDW-x state for Q_{hs} and Q_{an} are quite different, though neither exhibit a log. We have also tested the tb1 and tb4 dispersions of Ref. 28 and do not find any qualitative difference in our conclusions.

Convergence of eigenvalues

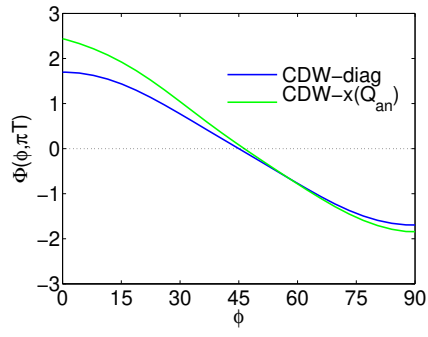


Supplementary Fig. 3: The dependence of the maximum eigenvalue on the grid size $N_k \times N_k$. These eigenvalues correspond to the CDW-diag state at 40 K. In each case, we use 16 Matsubara frequencies.

We have performed our calculations on a 101×101 momentum grid, which corresponds to a $0.02\pi/a$ momentum resolution. We checked different grid sizes and find that this grid is sufficient for convergence of the eigenvalues. Supplementary Fig. 3 shows the variation of eigenvalues as a function of the grid size. We also find that the number of Matsubara frequencies used in our calculation is sufficient for convergence of the eigenvalues in the temperature range that we study (40 K to 140 K).

Eigenvector projection on the Fermi surface

Here we show the projection of the eigenvector on the Fermi surface for the CDW-diag and CDW-x states. The full Brillouin zone dependence of these eigenvectors are shown in the main text (Fig. 3). On the Fermi surface, the CDW-diag state is well described by a $\cos 2\phi$ function, where ϕ is the angle along the Fermi surface. The bond oriented CDW-x state can be fit with $a + b \cos 2\phi + c \cos 4\phi$, where these terms represent the s , d , and s' components, respectively, with the d component the dominant contribution.



Supplementary Fig. 4: The dependence of the eigenvector corresponding to the leading eigenvalue for the ordering vectors (Q_{hs}, Q_{hs}) , and $(Q_{an}, 0)$, projected on the Fermi surface, where $\phi = 0$ corresponds to the antinodal point. This is shown for the lowest Matsubara frequency at $T=40$ K.